Fouling mechanisms of soluble microbial products and biomacromolecules extracted from membrane bioreactors during early filtration stages

Xinying Su[a,*], Rongjun Su[a,*], Zhigang Zhang[b], Yu Tian[c]

[a]Department of Environmental Engineering, School of Food Engineering, Harbin University of Commerce, Harbin 150076, China, Tel./Fax: +86 451 8460 0359; emails: suxinyinghit@163.com (X. Su), 765806356@qq.com (R. Su)
[b]Science and Technology on Underwater Acoustic Laboratory, College of Underwater Acoustic Engineering, Harbin Engineering University, Harbin 150001, China, email: zhigang.zhang@hrbeu.edu.cn
[c]State Key Laboratory of Urban Water Resource and Environment, Harbin Institute of Technology (SKLUWRE, HIT), Harbin 150090, China, email: hittianyu@163.com

abstract

A clear identification of the fouling mechanisms in membrane bioreactor can give a better understanding on membrane fouling. In this study, early filtration behaviors of soluble microbial products (SMP) and biomacromolecules (BMM) were compared and fouling mechanisms were investigated by Hermia's model. The results suggested that intermediate blocking, standard blocking, and complete blocking occurred successively for SMP filtration while intermediate blocking and cake filtration were the main fouling mechanisms acted in succession for BMM filtration. Moreover, pore blocking made a major contribution to flux decline and resistance increase for both SMP and BMM filtration. The effective porosity was lower for BMM filtration. In addition, three-dimensional excitation–emission matrix fluorescence spectra demonstrated that the fouling layer formed by BMM was beneficial for the removal of foulants such as soluble microbial byproduct-like materials.

Keywords: Membrane bioreactor; Biomacromolecules; Soluble microbial products; Fouling mechanisms; Hermia's model

1. Introduction

Successful utilization of membrane bioreactors (MBRs) has been greatly limited by membrane fouling. Fouling deteriorates membrane performance and shortens membrane life, leading to the increase of operation, and maintenance costs [1]. Numerous studies in recent years have investigated the cause and control of membrane fouling. The results show that the factors affecting membrane fouling mainly originate from membrane properties, mixture characteristics, and operating parameters [2]. Although substantial progress has been made, operational data from both full scale applications and laboratory studies reveal that membrane fouling is inevitable, and the fouling rate could be greatly reduced if managed appropriately [3].

One important reason that membrane fouling cannot be eliminated is that the mixture in MBRs contains particles ranging from nanometers (macromolecular assemblages) to hundreds of micrometers (bacterial aggregates). Included in this large range are particles such as biomacromolecules (BMM), soluble microbial products (SMP), colloids, and activated sludge flocs. Activated sludge flocs are relatively easily removed by the application of shear, while BMM, SMP, and colloids are much less influenced by shear effects and tend to dominate long-term fouling of membranes [3]. Colloids could be removed by physical cleaning while frequent physical cleaning affects the normal production of MBR. BMM and SMP are a pool of complex organics derived from substrate metabolism, biomass growth, and biomass decay during biological wastewater treatment [4,5]. Usually, SMP refer to soluble compounds and colloids <0.45 μm, while BMM refer to the soluble compounds, colloids, and particulates <10 μm.

* Corresponding author.

Due to the fact that the large-molecular weight compounds (0.45–10 μm) also play an important role in membrane fouling, the BMM solution has attracted much attention in recent studies [5–8].

Numerous research efforts have been made in the effect of size, composition, hydrophobic/hydrophilic, etc., on the fouling propensity of SMP and BMM [5,9–13]. Moreover, filtration and characterization of SMP have been studied to get a deeper understanding of flux decline and membrane retention [4,14,15] and some attention has been paid to the pore blocking mechanisms of SMP fraction (such as utilization-associated products, biomass-associated products, and hydrophilic substances) described by classical filtration models [16,17]. Mathematical treatment of flux decline has proved to be a useful tool in diagnosing filtration data [18]. However, in most instances, the flux decline data for SMP filtration are described by only one of the fouling mechanisms.

Moreover, the data corresponding to the early filtration stages do not follow the linear dependence, implying that the data might fit different blocking laws in succession. In the MBR, a rapid flux decline is expected to occur during the early filtration stages. The rate of fouling then decreases before reaching a plateau [19]. The deposition of BMM/SMP during the early filtration stages is the most likely reason of irreversible fouling [20,21]. A clear identification of the fouling mechanisms of SMP and BMM in the course of microfiltration (MF) could give a better understanding on membrane fouling. Modeling the flux decline during filtration could provide predictive tools for successful operation of a MF system [21]. To the best of our knowledge, little is known about the transition between fouling phenomena of SMP and BMM in early filtration stages.

Therefore, this study aims at a better understanding of the early fouling of SMP and BMM. Stirred dead-end filtration experiments were conducted to identify the differences between early filtration of SMP and BMM. The type and the relative importance of different fouling mechanisms were identified by fitting classical fouling models (linear formation) to the flux data by the linear least-square fitting. Then, the information derived from multistage Hermia's models can be used to investigate the chronological sequence/transition period of different fouling mechanisms. The effective porosity was estimated to identify the changes on membrane surfaces for SMP and BMM filtration. The retention of fresh and fouled membranes was also investigated to further confirm the significance of membrane property changes during fouling.

2. Materials and methods

2.1. Operation of MBR

A lab-scale 8 L MBR was operated at room temperature 22°C ± 3°C. The MBR was installed with a submerged MF membrane made of hollow fiber of polyvinylidene fluoride (PVDF). The MF membrane module is characterized with a nominal pore size of 0.1 μm and a filtration area of 0.1 m^2 (Motian, China).

The MBR was fed with synthetic municipal wastewater (glucose 227 mg/L; starch 227 mg/L; NaHCO$_3$ 254 mg/L; urea 33 mg/L; (NH$_4$)$_2$SO$_4$ 121 mg/L; KH$_2$PO$_4$ 15.4 mg/L; K$_2$HPO$_4$ 19.6 mg/L; and trace elements) from a wastewater tank; a liquid level control was used to control the water level in the bioreactor. The MBR was operated under constant flux and the effluent was controlled by a peristaltic pump. Aeration was provided continuously underneath the membrane module. Flux, temperature, pH, and transmembrane pressure (TMP) were regularly monitored. The membrane module was operated at the constant flux of 10 L/m^2 h with an intermittent suction of 8 min on and 2 min off. The hydraulic retention time was set at 10 h and the sludge retention time was maintained at 40 d. When the TMP reached 30 kPa, the membrane module was taken out. Then, chemical cleaning of the membrane module was carried out by soaking for 2–8 h in a 0.5% sodium hypochlorite solution. The MBR was operated for over 150 d.

2.2. Extraction and properties of SMP and BMM

The collected samples of activated sludge in MBR were centrifuged at 4,000 rpm for 5 min and then the extracted supernatant was collected. The extracted supernatant was filtered through filter paper (10 μm) and the filtrate was regarded as BMM, which includes colloidal, soluble compounds and perhaps some microorganisms [5]. A part of the filtrate was further filtered through a 0.45 μm membrane filter and was regarded as SMP. The SMP and biopolymers were analyzed for their protein and carbohydrates contents. The particle-size distributions of the SMP and BMM were obtained using Mastersizer 2000 and Malvern Zetasizer Nano (Malvern Co., UK) and shown in Fig. 1.

2.3. Filtration experiments

Filtration experiments were performed at a constant TMP (7.5 kPa) using a stirred dead-end membrane filtration cell at room temperature. The stirring speed in the cell was set at 200 rpm throughout the experiments. The membranes employed for filtration in this study were PVDF membrane with a nominal pore size of 0.22 μm (Lubitech, China). The permeate flux was recorded continuously. Before experiment, 1 L of ultrapure water was filtered.
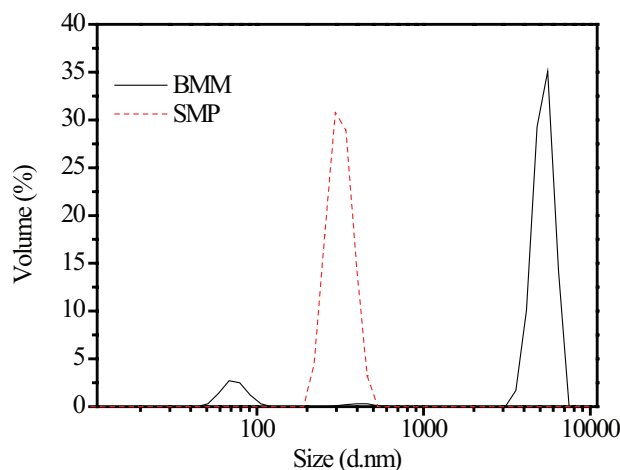

Fig. 1. The size distributions of SMP and BMM.

Then, clean water permeate flux was recorded to determine the pure water flux of the compacted membrane. Finally, each sample was poured into the cell and the filtration experiments stopped when the preset time was reached. In this study, the flux decline of both BMM and SMP reached a plateau after 6,000 s filtration based on preliminary experiments, and 6,000 s was chosen as the preset time of the early filtration stage.

Each sample was diluted to the same COD level (COD = 20 mg/L) to exclude the concentration effect. Considering the effects of residual deionized water the initial 10 mL of the filtrate was discarded. Then, 30 mL of permeate was taken as the initial filtrate. About 30 mL of permeate at the final stage of filtration was taken as the final filtrate.

2.4. Determination of fouling mechanisms

Hermia's models are derived from classical constant pressure dead-end filtration equations, which considered two types of fouling: pore blocking and cake layer formation. A general form of the Hermia's models can be expressed as:

$$\frac{d^2t}{dV^2} \alpha \left(\frac{dt}{dV}\right)^n \tag{1}$$

where t is time and V is volume filtered. The values of n are 0, 1, 3/2, and 2 for the cake, intermediate, standard, and complete blocking models, respectively [22]. Membrane fouling mechanisms could be described by four blocking filtration laws [23]: (1) complete pore blocking, that is, pore sealing; (2) standard pore blocking, that is, pore constriction; (3) intermediate pore blocking; and (4) cake filtration. The equations describing the four fouling mechanisms are summarized in Table 1.

Multistage fouling mechanisms were also determined in this study to better understand the fouling process. The main procedures for determination of the multistage filtration mechanisms [21] were as follows: (1) a portion filtration data ("core") that fits one of the linear equations in Table 1 with a coefficient of determination higher than 0.99 was identified; (2) the "core" was expanded by evaluating if a data point immediately adjacent to the "core" belonged to the 95% confidence interval based on the linear fit. The data point within the interval was included into the "core". The process was stopped when the data point was found to be located outside of the interval.

The data fitting processes were implemented with Matlab 7.7.0 (The MathWork Inc., USA).

2.5. Determination of the effective porosity

Based on Darcy's law, the hydraulic resistance of the fouling at a constant TMP can be determined by:

$$R_f = \left(\frac{J_0 - J}{J}\right) R_m \tag{2}$$

where R_m is the hydraulic resistance of clean membrane, J_0 and J are the initial and instantaneous values of the permeate flux, respectively. The hydraulic resistance of the fouling, R_f, can be estimated using Kozeny–Carman equation [21]:

$$R_f = \left[\frac{180(1-\varepsilon)}{\rho_p d_p^2 \varepsilon^3}\right] \frac{M_p}{A} \tag{3}$$

where A is the filtration area of membrane, ε is the effective porosity of the particle deposit, d_p and ρ_p are the diameter and the density of the foulants, respectively, M_p is the mass of foulants deposited on membrane surface. M_p is calculated based on the concentration and volume of the feed and permeate solution. Combining Eqs. (2) and (3), ε, can be determined with Matlab 7.7.0 (The MathWork Inc., USA).

2.6. Chemical analysis

Carbohydrates were determined according to the phenol–sulfuric acid method [24] with glucose as the standard. Proteins were determined by the modified Lowry method [25] with bovine serum albumin as the standard. All the above analyses were conducted in triplicate and the average values were reported. Particle-size distribution of the SMP and BMM was obtained by a laser granulometer (Mastersizer 2000, Malvern Co., UK). Excitation–emission matrix (EEM) spectra (FP 6500, JASCO, Japan) were collected

Table 1
Classical governing equations for flux decline at constant pressure derived from Hermia's models [23]

Fouling mechanisms	Flux equation	Total permeate volume equation	Linearized form
Complete blocking	$J = J_0 e^{-At}$	$V = \frac{J_0}{A}[1 - e^{-At}]$	$\ln J = \ln J_0 - k_1 t$
Standard blocking	$J = \frac{J_0}{(1 + Bt)^2}$	$V = \frac{J_0 t}{1 + Bt}$	$\frac{1}{\sqrt{J}} = f + gt$
Intermediate blocking	$J = \frac{J_0}{1 + At}$	$V = \frac{J_0}{A}\ln(1 + At)$	$\frac{1}{J} = \frac{1}{\beta} + \frac{k_c}{\beta}t$
Cake filtration	$J = \frac{J_0}{\sqrt{1 + Ct}}$	$V = \frac{2J_0}{C}[\sqrt{1 + Ct} - 1]$	$\frac{1}{J^2} = \frac{1}{J_0^2} + k_c t$

Note: J, flux; J_0, initial flux; V, filtrated volume; t, filtration time; A, B, and C are the constants; K is the constant with the subscript indicating the blocking mechanism, respectively.

with corresponding scanning emission spectra from 220 to 550 nm at 2 nm increments by varying the excitation wavelength from 220 to 400 nm at 5 nm sampling intervals.

3. Results and discussion

3.1. Fouling propensity of the BMM and SMP

Filtration experiments were performed to provide a basic understanding of fouling behavior of SMP and BMM. Fig. 2(a) shows the various permeate flux of SMP and BMM as a function of filtration time. In the initial filtration stage, the flux reductions for both SMP and BMM were very fast. For BMM, the initial filtration flux declined rapidly and the flux gradually reached a pseudo-steady state after 1,000 s. For SMP, membrane flux continued to decline and the flux decline slowed down significantly after 1,000 s. As shown in Fig. 2(a), the fouling potential of BMM was larger than that of SMP and the fastest fouling happened in the early filtration stages for the both SMP and BMM filtration.

The various hydraulic resistances during filtration of SMP and BMM as a function of filtration time are shown in Fig. 2(b).
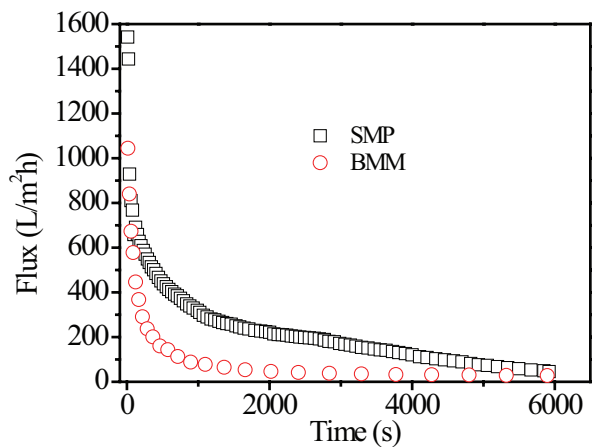
a)
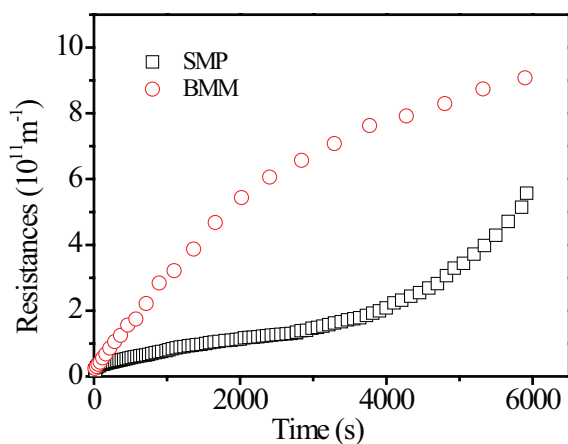
b)

Fig. 2. Time courses of (a) filtration flux and (b) hydraulic resistances during dead-end filtration of SMP and BMM (filtration pressure: 7.5 kPa).

The hydraulic resistances for BMM filtration were always higher than those for SMP filtration throughout the filtration process. However, the increases of hydraulic resistances for SMP and BMM filtration exhibited different trends. For SMP, the increase rate of hydraulic resistance at the beginning was 3.9×10^7/m·s, followed by a higher value of 17.1×10^7/m·s after about 4,000 s. For BMM, a faster increase rate of hydraulic resistance was detected as 27.1×10^7/m·s at the beginning, and the hydraulic resistance decline slowed down significantly (9.1×10^7/m·s) after approximate 2,000 s. The difference for the increases of hydraulic resistances between SMP and BMM filtration might be due to the different membrane fouling mechanism caused by SMP and BMM.

3.2. Blocking mechanisms of the BMM and SMP

Linearized forms of individual classical model were applied to preliminary determine if they would provide better fits of the experimental data. Fig. 3 illustrates the data (symbols points) and model fits (lines). The coefficients of determination (R^2) for the different models were supplied in Fig. 3 to allow a comparison of the different models. For the SMP filtration, it can be observed that besides complete blocking model ($R^2 = 0.9605$), standard blocking model could result in a high R^2 value (0.9556) as well, implying standard blocking might also be the fouling mechanism of SMP. For the BMM filtration, the cake filtration model showed the most excellent fit ($R^2 = 0.9920$) to experimental data, suggesting that the fouling mechanism of BMM was mainly attributed to cake filtration.

However, the single model data fitting did not reveal the trends of experimental data although the corresponding R^2 values were up to 0.9667 or even 0.9920. Therefore, the fitting adopted single model did not reveal the filtration mechanism exactly. It is reasonable to consider that one or several of these blocking mechanisms occurred simultaneously or sequentially. A clear identification of the differentiation among the mechanisms has important implications for the optimal choice of the membrane, suppression of membrane fouling and decision of membrane cleaning strategy. Therefore, a multistage data fitting, which assumes that different mechanisms dominate at different filtration time, was employed to investigate the fouling process of SMP and BMM in more detail [21].

Fig. 4 shows the time sequence of dominant fouling mechanisms occurring in early filtration SMP and BMM exploited multistage data fitting. It is noted that there was a transition phase of each fouling mechanism that occurred during the filtration, suggesting two fouling mechanisms acted simultaneously at the transition time. With respect to SMP filtration, intermediate blocking occurred first, followed by standard blocking, and then complete blocking after about 2,700 s. Regarding BMM filtration, intermediate blocking and then cake filtration (after about 2,020 s) were found to occur successively in filtration experiments. Given the presence of large surface pores (0.22 μm) in the membranes, pore blocking clearly occurred at the beginning of the filtration for both SMP and BMM. Then, cake filtration dominated for filtration of the BMM probably due to the larger size of BMM.

Furthermore, the percentages of flux decline corresponding to different fouling mechanisms were evaluated
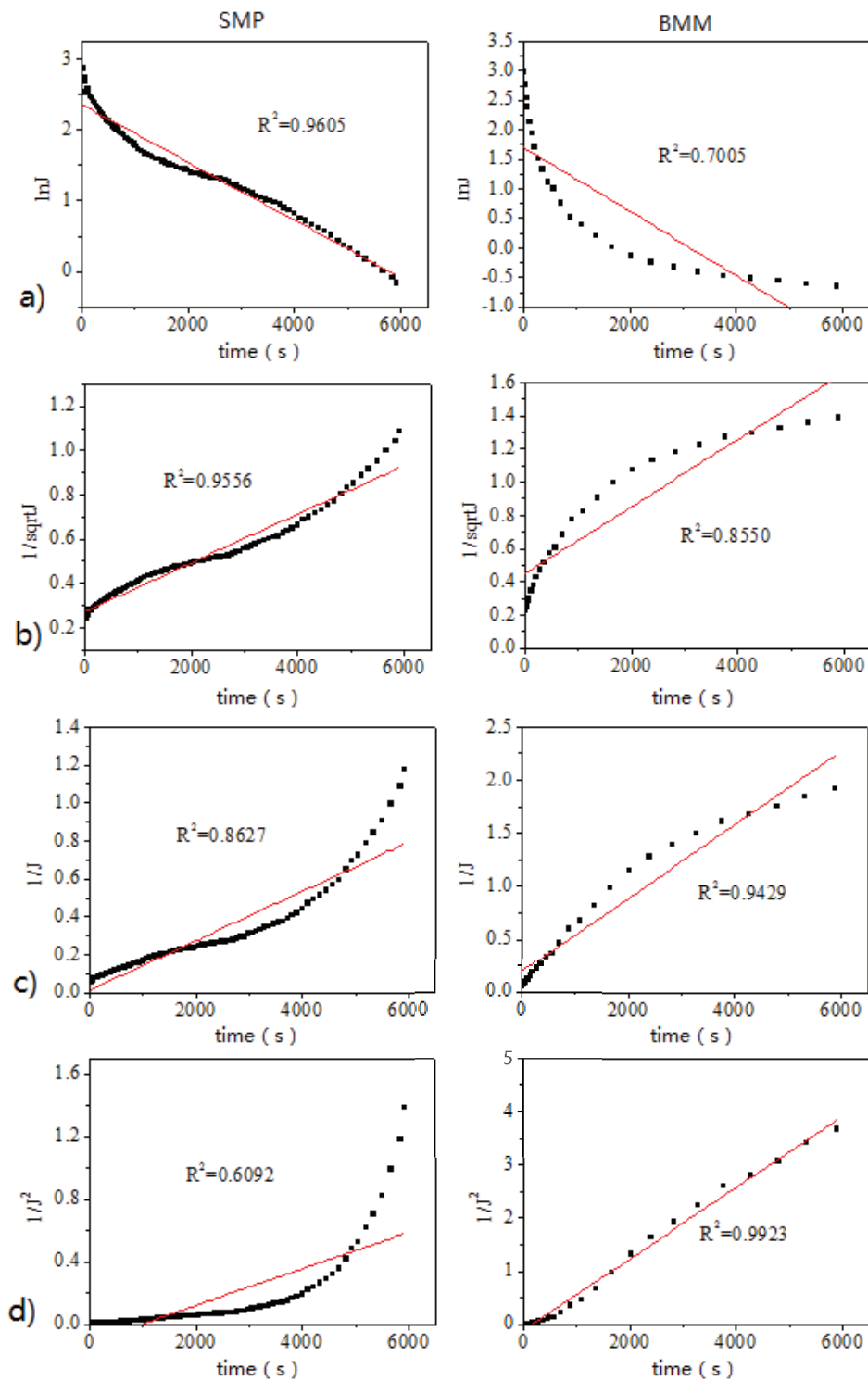
Fig. 3. Fitting the flux decline data to the four blocking mechanisms models: (a) complete blocking, (b) standard blocking, (c) intermediate blocking, and (d) cake filtration.

to identify the relative importance of different fouling mechanisms (shown in Table 2). With respect to SMP filtration, time durations occupied by intermediate blocking, standard blocking, and complete blocking were 30.3%, 20.1%, and 54.4%, respectively. Referring to BMM filtration, the longest time was for cake filtration, which accounted for 65.7% of the total filtration time. For both SMP and BMM filtration, intermediate blocking made a major contribution to flux decline, which resulted in 85.1% and 95.6% of flux decline with only 30.3% and 34.3% of filtration time, respectively. It was noted
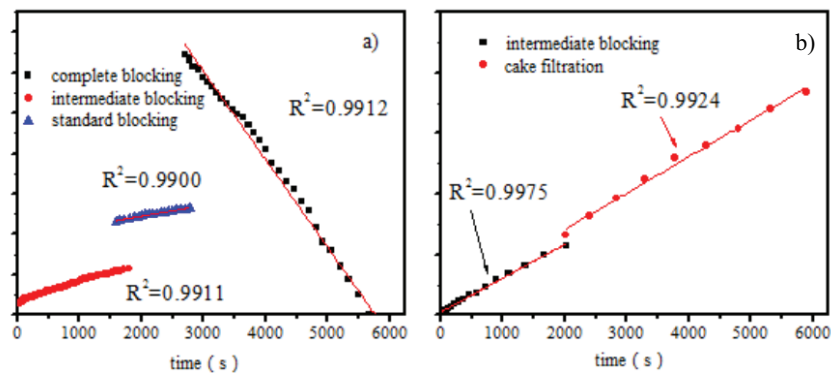
Fig. 4. The multistage filtration mechanisms in terms of (a) SMP and (b) BMM.

Table 2
The distributions and contributions of the blocking mechanisms in terms of time and percentage of flux decline

Blocking mechanisms (in terms of time)	Intermediate blocking	SMP		BMM	
		Standard blocking	Complete blocking	Intermediate blocking	Cake filtration
The distribution of time (%)	30.3	20.1	54.4	34.3	65.7
The distribution of flux decline (%)	85.1	3.6	9.5	95.6	1.8

that for BMM filtration, more than 65.7% of filtration time corresponded to the mechanism of cake filtration induced only less than 1.8% of the flux decline, that is, the contribution of cake filtration to the flux decline was much less than that of pore blocking. These values were conservative estimate. In practical situation, the longer the filtration time of the experiment was, the more remarkable the differences in the overall contribution to flux decline were brought by the cake filtration and pore blocking. Combined the changes of resistance (Fig. 2(b)), it can be obtained that complete blocking contributed the most to the increase of resistance for SMP filtration while cake filtration devoted the least for BMM filtration. Therefore, it can be inferred that pore blocking is a major contributor to the flux decline and resistance increase.

3.3. Changes of surface properties of membranes

The estimation of the effective porosity demonstrated that the variations of the effective porosity were rather different. The effective porosity for SMP filtration increased initially for about 400 s and then kept a relatively steady value (Fig. 5). This result was similar with the observation of Wang and Tarabara [21], implying that with the filtration of SMP an initially loose deposit developed into a more compact one until the formation of a stable and uniform fouling layer. From 3,000 s to the end, the effective porosity continued to reduce. However, with respect to BMM filtration, the effective porosity decreased throughout the whole filtration phase and then was stable at around 0.22. It also can be seen from Fig. 5 that the effective porosity for SMP filtration was always higher than that for BMM filtration, suggesting the presence of
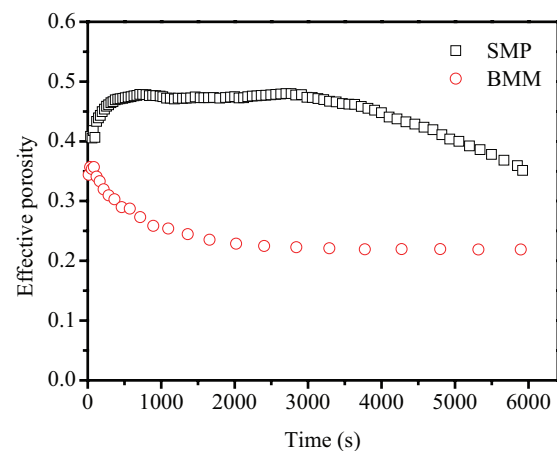

Fig. 5. Effective porosity of the layer of SMP and BMM deposited onto the surface of membranes.

colloidal substance in BMM can block the membrane pore directly, leading to a serious decline in porosity during initial filtration stages.

3.4. Retention behaviors of fresh and fouled membranes

The retention of fresh and fouled membranes was also investigated. The concentrations of carbohydrates and proteins fractions in SMP, BMM, and their corresponding permeate including initial and final filtrate are shown in Fig. 6.

For both SMP and BMM, the content of carbohydrates was the predominant fraction and almost twice as that of proteins. According to the different extraction conditions,
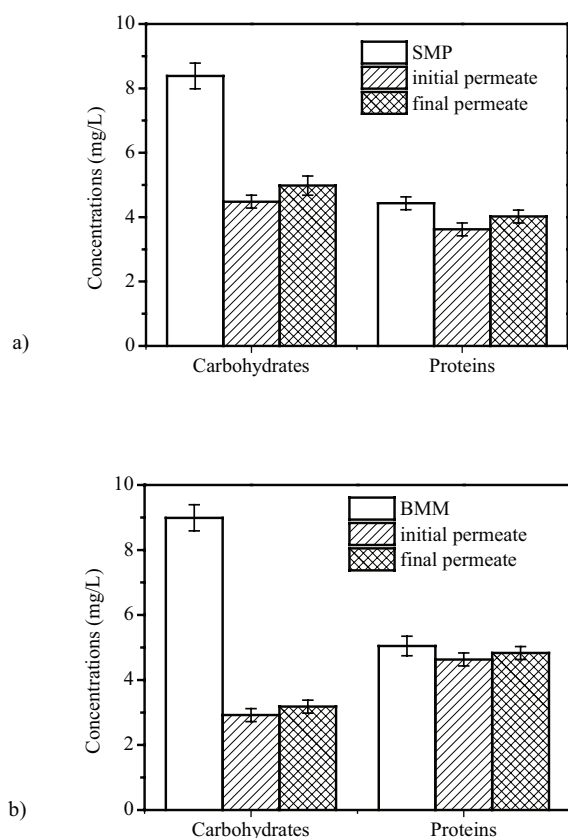
Fig. 6. (a) SMP and (b) BMM concentration in raw, initial, and final permeate.

BMM contained SMP, colloidal substances, and some cells. With respect to the SMP filtration, the carbohydrates content was 8.4 ± 0.4 mg/L, and the initial and final permeate carbohydrates concentrations were 4.5 ± 0.2 and 5.0 ± 0.3 mg/L, respectively. The proteins content in SMP was 4.4 ± 0.2 mg/L, and the initial and final permeate proteins concentrations were 3.6 ± 0.2 and 4.0 ± 0.2 mg/L, respectively. As for the BMM filtration, the carbohydrates and proteins content were 9.0 ± 0.4 and 5.0 ± 0.3 mg/L, respectively. The corresponding carbohydrates and proteins concentrations in initial permeate were 2.9 ± 0.2 and 4.6 ± 0.2 mg/L, and those in final permeate were 3.2 ± 0.2 and 4.8 ± 0.2 mg/L, respectively. It can be seen that the retention of membrane on SMP and BMM were different. The membrane retention for BMM filtration was better than that for SMP filtration, especially for carbohydrates fraction ranging from 40.6% to 67.5%. Analogously, proteins were also retained by the membrane, ranging from 4.4% to 18.3%. The possible reason might be the colloid in BMM formed a relatively dense contamination layer on the membrane surface, and this layer acted as a secondary barrier resulting in improved effluent quality.

It is worth noting that the concentrations of carbohydrates and proteins in the final permeate were a little higher than those in the initial permeate. This difference might be attributed to the adsorption process of the membrane. In the early stage of membrane filtration, the contaminant removal included retention and adsorption. The adsorption became saturated with the extension of time, while the retention of

contamination layer formed on the surface of membrane gradually strengthened over time. As shown in Fig. 6, the contaminant removal in final filtration was worse than that in initial filtration, suggesting that the adsorption ability of membrane was greater in this study.

Three-dimensional EEM fluorescence spectra of the SMP, BMM, and their initial and final permeate are illustrated in Fig. 7. For the SMP samples, three peaks were identified at Ex/Em 280/350, 250/425, and 320/410 nm, which were related to soluble microbial byproduct-like materials (Peak A), fulvic-acid like substances (Peak B), and humic-like substances (Peak C) [26,27]. Wang et al. [28] demonstrated that the Peak A appeared in the EEM fluorescence spectra of membrane foulants. After membrane filtration, the fluorescent intensities of soluble microbial byproduct-like materials (Peak A) in initial and final permeate were 441.5 and 460.6, respectively, showing the decrease compared with the SMP (483.5). These results suggest that for the SMP filtration, the removal of soluble microbial byproduct-like materials in the initial filtration was superior to that in the final filtration, which might be ascribed to the adsorption of fresh membrane.

With respect to BMM, four main peaks were identified for all the samples. The fulvic-acid like substances (Peak B) and humic-like substances (Peak C) were the same as those in SMP, while the soluble microbial byproduct-like materials (Peak A) located at Ex/Em = 280/340. In addition, a significant peak at Ex/Em = 235/340 (Peak D) was identified as simple aromatic protein substances. After membrane filtration, simple aromatic protein substances were almost completely removed both for the initial and final permeate. While the fluorescence intensity of soluble microbial byproduct-like materials in the final permeate was less than those in the initial permeate, suggesting that the fouling layer formed on the membrane surface was beneficial for the further removal of soluble microbial byproduct-like materials. According to the mechanism analysis, the main fouling mechanism of BMM filtration was cake filtration, indicating that the BMM cake layer formed on the membrane surface. The function of membrane was efficient for the retention of simple aromatic protein substances, while the function of fouling layer was efficient for the retention of soluble microbial byproduct-like materials. Some studies have recognized that the fouling layer in membrane filtration acts as a secondary barrier to impurities in the feed stream resulting in improved effluent quality [3], which was in consistent with the results of this study. The fouling layer formed by BMM was beneficial for the removal of foulants such as soluble microbial byproduct-like materials and lead to more serious membrane fouling at the same time.

4. Conclusions

Multistage data fitting showed that intermediate blocking, standard blocking, and complete blocking occurred successively in SMP filtration, while intermediate blocking and cake filtration acted in succession in BMM filtration. Furthermore, pore blocking made a major contribution to flux decline and resistance increase for both SMP and BMM filtration. The BMM fouling made the effective porosity lower and membrane surface rougher. The membrane retention for BMM filtration was better than SMP filtration due to the fouling layer formed by BMM, which was beneficial for
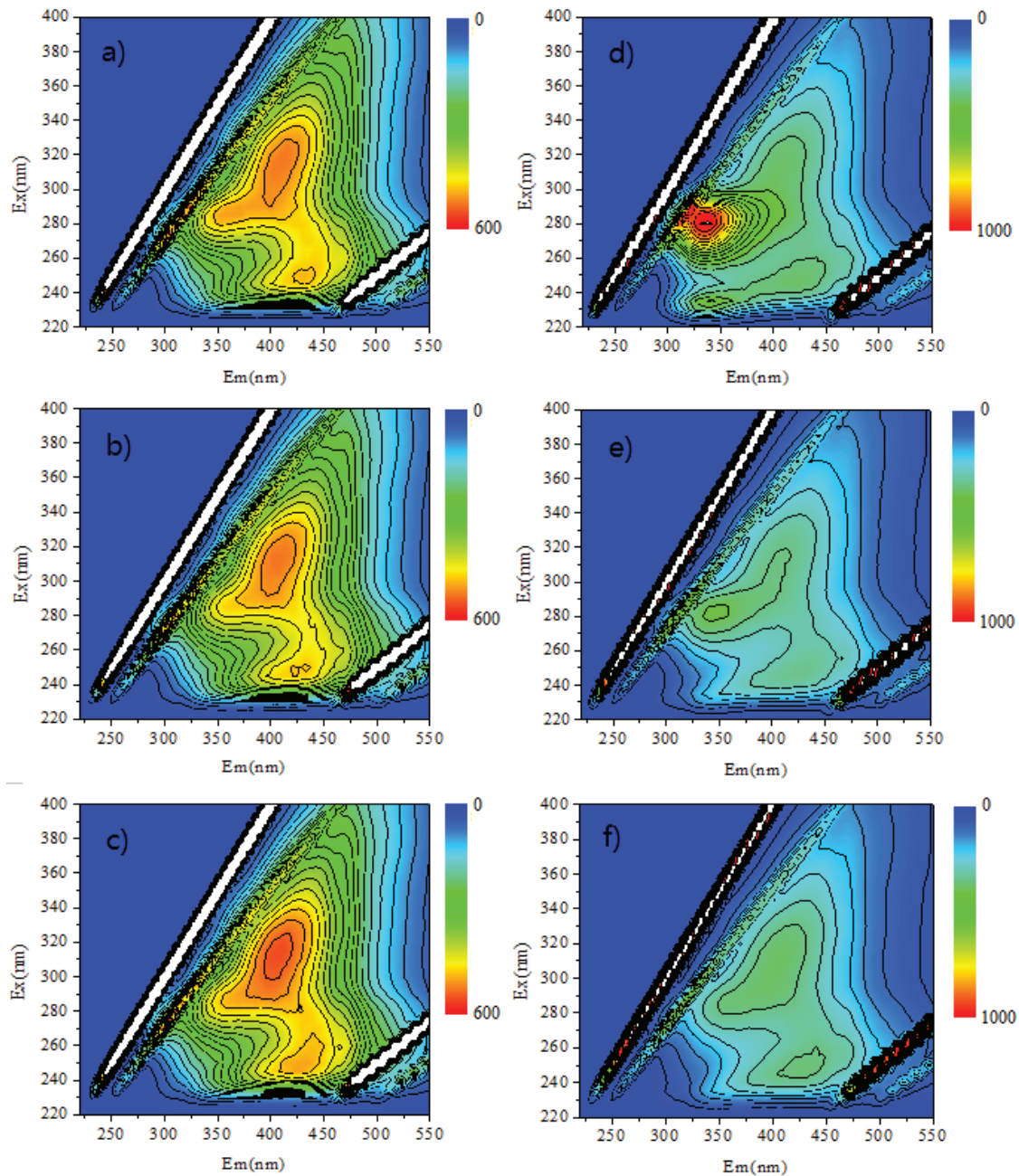
Fig. 7. EEM of (a) SMP in raw, (b) SMP in initial permeate, (c) SMP in final permeates, (d) BMM in raw, (e) BMM in initial permeate, and (f) BMM in final permeate.

the removal of foulants. Moreover, attributing to the adsorption of the fresh membrane, the contaminant removal in the initial filtration was better.

References

[1] D. Violleau, H. Essis-Tome, H. Habarou, J.P. Croue, M. Pontie, Fouling studies of a polyamide nanofiltration membrane by selected natural organic matter: an analytical approach, Desalination, 173 (2005) 223–238.
[2] H.M. Zhang, J.F. Gao, T. Jiang, D.W. Gao, S.R. Zhang, H.Y. Li, F.L. Yang, A novel approach to evaluate the permeability of cake layer during cross-flow filtration in the flocculants added membrane bioreactors, Bioresour. Technol., 102 (2011) 11121–11131.
[3] X.M. Wang, T.D. Waite, Impact of gel layer formation on colloid retention in membrane filtration processes, J. Membr. Sci., 325 (2008) 486–494.

[4] C. Jarusutthirak, G. Amy, Role of soluble microbial products (SMP) in membrane fouling and flux decline, Environ. Sci. Technol., 40 (2006) 969–974.

[5] F.G. Meng, Z.B. Zhou, B.J. Ni, X. Zheng, G. Huang, X. Jia, S. Li, Y. Xiong, M. Kraume, Characterization of the size-fractionated biomacromolecules: tracking their role and fate in a membrane bioreactor, Water Res., 45 (2011) 4661–4671.

[6] Z.B. Zhou, X. He, M.H. Zhou, F.G. Meng, Chemically induced alterations in the characteristics of fouling-causing bio-macromolecules – implications for the chemical cleaning of fouled membranes, Water Res., 108 (2017) 115–123.

[7] Z.B. Zhou, F.G. Meng, S.R. Chae, G.C. Huang, W.J. Fu, X.S. Jia, S.Y. Li, G.H. Chen, Microbial transformation of biomacromolecules in a membrane bioreactor: implications for membrane fouling investigation, Plos One, 7 (2012) 1–9.

[8] Z.B. Zhou, F.G. Meng, S. Liang, B.J. Ni, X.S. Jia, S.Y. Li, Y.K. Song, G.C. Huang, Role of microorganism growth phase in the accumulation and characteristics of biomacromolecules (BMM) in a membrane bioreactor, RSC Adv., 2 (2012) 453–460.

[9] A. Drews, Membrane fouling in membrane bioreactors—characterisation, contradictions, cause and cures, J. Membr. Sci., 363 (2010) 1–28.

[10] S. Rosenberger, C. Laabs, B. Lesjean, R. Gnirss, G. Amy, M. Jekel, J.C. Schrotter, Impact of colloidal and soluble organic material on membrane performance in membrane bioreactors for municipal wastewater treatment, Water Res., 40 (2006) 710–720.

[11] A. Drews, M. Vocks, U. Bracklow, V. Iversen, M. Kraume, Does fouling in MBRs depend on SMP?, Desalination, 231 (2008) 141–149.

[12] S. Liang, C. Liu, L.F. Song, Soluble microbial products in membrane bioreactor operation: behaviors, characteristics, and fouling potential, Water Res., 41 (2007) 95–101.

[13] J.Y. Tian, Z.L. Chen, H. Liang, X. Li, Z.Z. Wang, G.B. Li, Comparison of biological activated carbon (BAC) and membrane bioreactor (MBR) for pollutants removal in drinking water treatment, Water Sci. Technol., 60 (2009) 1515–1523.

[14] H.S. Shin, S.T. Kang, Characteristics and fates of soluble microbial products in ceramic membrane bioreactor at various sludge retention times, Water Res., 37 (2003) 121–127.

[15] F.G. Meng, A. Drews, R. Mehrez, V. Iversen, M. Ernst, F.L. Yang, M. Jekel, M. Kraume, Occurrence, source, and fate of dissolved organic matter (DOM) in a pilot-scale membrane bioreactor, Environ. Sci. Technol., 43 (2009) 8821–8826.

[16] Y.X. Shen, W.T. Zhao, K. Xiao, X. Huang, A systematic insight into fouling propensity of soluble microbial products in membrane bioreactors based on hydrophobic interaction and size exclusion, J. Membr. Sci., 346 (2010) 187–193.

[17] Y. Tian, L. Chen, S. Zhang, S. Zhang, A systematic study of soluble microbial products and their fouling impacts in membrane bioreactors, Chem. Eng. J., 168 (2011) 1093–1102.

[18] N.G. Cogan, S. Chellam, Incorporating pore blocking, cake filtration, and EPS production in a model for constant pressure bacterial fouling during dead-end microfiltration, J. Membr. Sci., 345 (2009) 81–89.

[19] P. Le-Clech, V. Chen, T.A.G. Fane, Fouling in membrane bioreactors used in wastewater treatment, J. Membr. Sci., 284 (2006) 17–53.

[20] H. Choi, K. Zhang, D.D. Dionysiou, D.B. Oerther, G.A. Sorial, Effect of permeate flux and tangential flow on membrane fouling for wastewater treatment, Sep. Purif. Technol., 45 (2005) 68–78.

[21] F. Wang, V.V. Tarabara, Pore blocking mechanisms during early stages of membrane fouling by colloids, J. Colloid Interface Sci., 328 (2008) 464–469.

[22] J. Hermia, Constant pressure blocking filtration law: application to power law non-Newtonian fluids, Chem. Eng. Res. Des., 60 (1982) 183–187.

[23] W.R. Bowen, J.I. Calvo, A. Hernández, Steps of membrane blocking in flux decline during protein microfiltration, J. Membr. Sci., 101 (1995) 153–165.

[24] M. Dubois, K.A. Gilles, J.K. Hamilton, P.A. Rebers, F. Smith, Colorimetric method for determination of sugars and related substances, Anal. Chem., 28 (1956) 350–356.

[25] O.H. Lowry, N.J. Rosebourgh, A.L. Farr, R.J. Randall, Protein measurement with the folin phenol reagent, J. Biol. Chem., 193 (1951) 265–275.

[26] W. Chen, P. Westerhoff, J.A. Leenheer, K. Booksh, Fluorescence excitation–emission matrix regional integration to quantify spectra for dissolved organic matter, Environ. Sci. Technol., 37 (2003) 5701–5710.

[27] A. Baker, Fluorescence excitation–emission matrix characterization of some sewage-impacted rivers, Environ. Sci. Technol., 35 (2001) 948–953.

[28] Z.W. Wang, Z.C. Wu, S.J. Tang, Characterization of dissolved organic matter in a submerged membrane bioreactor by using three-dimensional excitation and emission matrix fluorescence spectroscopy, Water Res., 43 (2009) 1533–1540.